Chemical Engineering Science 104 (2013) 565–573

Contents lists available at ScienceDirect

Chemical Engineering Science

journal homepage: www.elsevier.com/locate/ces

Pore diffusion model to predict the kinetics of heterogeneous catalytic esterification of acetic acid and methanol

Mallaiah Mekala, Sunil Kumar Thamida, Venkat Reddy Goli *

Department of Chemical Engineering, National Institute of Technology, Warangal 506004, Andhra Pradesh, India

HIGHLIGHTS

- Indion180, a novel catalyst is used for esterification of acetic acid and methanol.
- A hybrid model of heterogeneous and homogeneous catalysis is developed.
- Convection–diffusion–reaction is solved inside the spherical catalyst particle.
- Linear dependence of initial reaction rate on catalyst loading is established.
- The kinetics is nearly independent of catalyst particle size.

ARTICLE INFO

Article history:
Received 25 May 2013
Received in revised form
16 September 2013
Accepted 23 September 2013
Available online 1 October 2013

Keywords:
Catalysis
Kinetics
Diffusion
Mathematical modeling
Simulation
Esterification

ABSTRACT

A novel pore diffusion model in combination with a homogeneous reaction in the bulk solution is proposed to model the kinetic behavior of conversion of acetic acid during its esterification with methanol using ion exchange resin catalyst. The model parameters are determined based on the experimental data of a batch reactor with reactant quantities in stoichiometric ratio. Experimental kinetic data of conversion of acetic acid is obtained for various ranges of parameters such as catalyst loading in g/cc of reactant mixture volume, temperature in the range of 323.15–353.15 K, average diameter of catalyst particle varied from 425 μm to 925 μm and RPM of magnetic stirrer. A multi time scale model is adopted in updating the conversion of acetic acid in the bulk liquid where the measurement is carried out. Since the homogeneous part of catalytic esterification is slow reaction, a large time step is used for updating bulk concentration or conversion, whereas a small time step is used to find the concentration distribution and inward flux of acetic acid inside the catalyst particle in a quasi steady state mode. This multi time scale approach leads to utilizing only the initial time kinetics of reaction for predicting two reaction constants namely k_{f1}, the forward reaction rate constant for homogeneous reaction in bulk solution and k_{f2}, the forward reaction rate constant for reaction inside the catalyst particle. The equilibrium conversion data provides the reaction equilibrium constant. The model predicts the overall kinetics of heterogeneous esterification reaction accurately.

1. Introduction

Organic esters are important chemicals and widely used in cosmetics, plasticizers, medicinal, polymerization, textile, flavors and food industries. Several synthetic chemical routes are available to produce these organic esters. In particular, methyl acetate manufactured commercially is in great demand. It is especially used as a solvent in adhesives, nail polish removers, paints, printing inks, perfumery, dye production and industrial coatings. One of the comprehensive reviews of esters synthesis is given by Yadav and Mehta (1994).

For esterification of acetic acid and methanol, the reaction could be represented by

$$CH_3COOH\ (A) + CH_3OH\ (B) \rightleftharpoons CH_3COOCH_3(C) + H_2O\ (D). \quad (1)$$

where acetic acid (A, CH_3COOH) and methanol (B, CH_3OH) react in liquid state to produce methyl acetate (C, CH_3COOCH_3) and water (D, H_2O). This reaction is primarily slow and reversible. To enhance the reaction rate, catalytic esterification is a major breakthrough in the field of esterification. One of the earliest works relating to kinetics of catalytic esterification of acetic acid with methanol was published by Rolfe and Hinshelwood (1934). Ronnback et al. (1997) investigated the kinetics of esterification of acetic acid with methanol using hydrogen iodide as homogeneous catalyst. It was observed that hydrogen iodide also reacted with methanol and produced methyl iodide as a by-product. Agreda et al. (1990)

* Corresponding author. Tel.: +91 870 2462602; fax: +91 870 2459547.
E-mail address: v.reddy@nitw.ac.in (V.R. Goli).

0009-2509/$ - see front matter © 2013 Elsevier Ltd. All rights reserved.
http://dx.doi.org/10.1016/j.ces.2013.09.039

proposed a rate expression for the esterification reaction using sulphuric acid as a homogeneous catalyst.

Solid catalyst such as ion exchange resins have been recently found to be very effective in improving the rate of reaction as well as in separation of products. Ion exchange resins are the most common heterogeneous catalysts used for esterification reaction (Yadav and Thathagar, 2002; Zhang et al., 2004; Chakrabarti and Sharma, 1993). The basic mechanism for using catalytic resin as catalyst is that they liberate H^+ ions which catalyze the esterification reaction (Jagadeesh Babu et al., 2011; Tsai et al., 2011; Lopez et al., 2008). This has been verified by using H_2SO_4 as a homogeneous catalyst (Liu et al., 2006). But using H_2SO_4 is uneconomical as there would be a further separation step involved for removing H_2SO_4 after the products are formed. Hence solid catalyst assisted esterification is preferred. Though acetic acid itself acts as a catalyst but its activity for reaction is slow due to its weak acidic nature. So addition of cat-ion ion exchange resin catalyst would provide more H^+ ions for catalyzing the reaction. Even for production purpose, solid catalyst could be used as packing for conducting catalytic reactive distillation in a packed column (Popken et al., 2001). In order to design a catalytic reactive distillation column, it requires a suitable kinetic model that accounts for catalyst influence. This type of heterogeneous esterification has been modeled by various approaches (Popken et al., 2000; Song et al., 1998; Yu et al., 2004; Kirbaslar et al., 2001a, 2001b; Winkler and Gmehling, 2006; Ehteshai et al., 2006). These models assumed various possibilities such as pseudo homogeneous, surface reaction and adsorption steps. But, all these models predict the kinetics by fitting adjustable parameters in terms of catalyst loading and temperature. In this paper, a novel pore diffusion model is proposed where a major conversion of reactants occurs inside the catalyst pore. The novel model explicitly accounts for temperature, catalyst loading and diameter of the catalyst particle.

2. Experiments

2.1. Chemicals

The reactants used are methanol (purity=99% w/w) and acetic acid (purity=99.95% w/w) supplied by SD Fine Chemicals Ltd. (Mumbai, India).

2.2. Catalyst

The solid acid catalyst used for the esterification reaction is Indion 180 supplied by Ion-Exchange India Limited, Mumbai, India. Indion 180 has cross-linked three-dimensional structures of polymeric material obtained by sulfonation of a copolymer of polystyrene and divinylbenzene (DVB). It is in the form of an opaque and dark gray colored solid spherical bead. The resins used in this study were dried for two hours in a hot air oven at temperature 90 °C to remove the moisture content. The properties of the resin catalyst as given by the supplier are shown in Table 1. A snapshot of the catalyst particles is shown in Fig. 1. The catalyst particles may not be mono-disperse but there would be a small size range since the particles are segregated using a sieve. The size range is the difference between the pore sizes of the successive sieve plates. For a particular case of the 425 μm, the above and below sieve pores have a size of 500 μm and 350 μm, respectively. The remaining size ranges are 1000–850 μm (average size is 925 μm) and 850–600 μm (average size is 725 μm).

2.3. Experimental setup

A schematic diagram of the experimental setup is shown in Fig. 2. It consists of a 500 ml three neck round-bottom flask. The flask was placed in a heating rota-mantle which has a heat control knob and stirrer speed control knob. The rotational speed of magnetic stirrer was varied from 240 rpm to 640 rpm by using the speed control knob. A spiral condenser was connected to the reaction flask vertically to condense the vapor and mix them back with the reacting mixture. Vapor losses were reduced by provision of the condenser. The heating is controlled manually to maintain a desired temperature in the reaction flask. A thermometer is inserted into the flask to measure the reaction mixture temperature. Thus the rota-mantle was used to maintain constant temperature and constant stirring speed.

Table 1
Physico-chemical properties of Indion 180 catalyst.

Physical property	Indion 180
Manufacturer	Ion Exchange India Limited
Shape	Spherical beads
Physical form	Opaque, grey to dark grey coloured
Size (μm)	725
Apparent bulk density (g/cm^3)	0.55–0.60
Surface area (m^2/g)	28–32
Pore volume (ml/g)	0.32–0.38
Max. operating temperature (°C)	150
Hydrogen ion capacity, (meq/g)	5.0
Matrix type	Styrene-DVB
P^H range	0–7
Resin type	Macro porous strong acidic cat-ion
Functional group	$-SO_3^-$
Ionic form	H^+

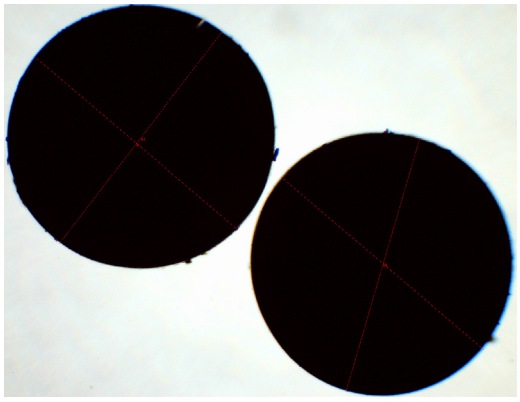

Fig. 1. Snapshot of catalyst particles displaying the sphericity.

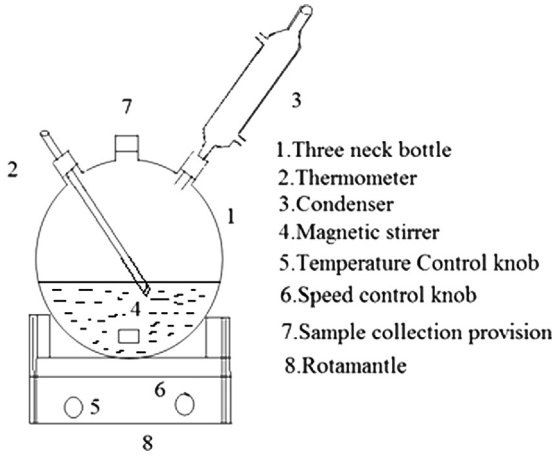

Fig. 2. Experimental setup for reaction kinetics studies.

2.4. Experimental procedure

In the experiments, equimolar quantities of liquid methanol (32 g) and liquid acetic acid (60 g) were mixed and charged to the reactor. The total volume of the bulk solution is 98 ml. This gives the initial concentration C_{A0} of acetic acid as 10.24 mol/l. The reaction mixture was heated to a desired temperature quickly within 4–5 min and a measured quantity of the catalyst particles was added to the reaction mixture. The volume of catalyst would be 1.97 cc for a catalyst loading of 0.025 g/cc. There might be a minute conversion of reactants during this time period but the major reaction rate picks up only after addition of catalyst (Popken et al., 2000; Jagadeesh Babu et al., 2011). The time is also recorded from the point of addition of the catalyst. Samples of the reaction mixture were withdrawn at regular intervals of time and titrated with 0.1 N NaOH solution prepared in distilled water for finding the acetic acid concentration. The reaction was carried out for sufficient time so that equilibrium conversion is reached or when no further decrease of acetic acid concentration takes place. The equilibrium is reached in about 3–4 h depending on catalyst loading and temperature.

2.5. Chemical analysis

Water used in the experiment to prepare the standard solution of NaOH was obtained from an ultra pure water purifier system (Millipore-Synergy UV system). The resistance of water is recorded as 18.2 MΩ-cm. The acetic acid concentration (C_{Ab}) in sample taken from reactant mixture was determined by titration of sample against standard 0.1 N solution of NaOH using phenolphthalein as the indicator. The endpoint is indicated by pale pink color.

2.6. Experimental data

Esterification reaction with Indion 180 as solid catalyst was investigated with 1:1 mol ratio of acetic acid and methanol. The reaction conditions were varied sufficiently to acquire data on conversion kinetics. The stirrer speed was varied from 240 RPM to 640 RPM. The temperature was varied from 323.15 K to 353.15 K. The catalyst loading was varied from 0.01 g/cc to 0.05 g/cc based on initial reaction mixture. The average diameter of the catalyst particles was varied from 425 μm to 925 μm. The effect of intrinsic reaction condition such as temperature and practical settings such as catalyst loading, stirrer speed and catalyst particle size on the reaction kinetics is discussed below.

2.6.1. Effect of reaction temperature

The experimental data obtained at different temperatures shown later in Fig. 10 along with model prediction for a fixed catalyst loading of 0.025 g/cc shows that the rate of conversion of acetic acid increases with an increase in the temperature. This indicates that the reaction rate is controlled by temperature to some extent. Higher the temperature less is the time taken for the system to reach equilibrium.

2.6.2. Effect of catalyst loading

Experiments were carried out with different catalyst loading ranging from 0.01 g/cc to 0.05 g/cc. The experimental results obtained with different catalyst loading at a fixed temperature show that as the catalyst loading increases the rate of reaction increases as shown later in Fig. 9 along with the model prediction. When the amount of catalyst in the reaction mixture is increased, the reaction rate increases because of more H^+ ions being provided by the catalyst.

2.6.3. Effect of stirrer speed

To study the effect of external mass transfer resistance on the esterification reaction, experiments were conducted at different stirrer speeds ranging from 240 RPM to 640 RPM. Other experimental conditions were: initial mole ratio of reactants equal to 1:1, diameter of catalyst as 725 μm, catalyst loading of 0.025 g/cc and temperature of 343.15 K. Fig. 3 shows the kinetics of conversion of acetic acid at different agitation speeds. From this experimental data it can be seen that the conversion of acetic acid is not affected by the stirrer speed beyond 240 RPM. This indicates that the external mass transfer resistance is negligible for agitation speed greater than 240 RPM. The present results are in good agreement with literature results (Titus et al., 2007; Ali et al., 2007; Mao et al., 2008; Delgado et al., 2007; Cruz et al., 2007).

2.6.4. Effect of catalyst particle size

Experiments were carried out with different particle sizes and surprisingly there is only a marginal increase of reaction rate with decrease in particle size as shown along with model prediction in Fig. 11. The experimental data provides the evidence that the diameter of particle has only little effect on the rate of reaction while keeping the same catalyst loading. This is an interesting feature because if one considers that heterogeneous reaction occurs only on the surface of the catalyst particle then the available specific surface area per unit volume of reactant solution goes as $\sim 1/R_p$ and the reaction rate should increase substantially with decrease in particle size. But, our model would incorporate a new assumption that the heterogeneous reaction occurs in inside of the catalyst particle also. The resultant dependence of reaction rate on catalyst particle size has to be obtained only after solving the reaction-diffusion equation inside the catalyst particle.

The internal reaction and diffusion are fast compared to the bulk homogeneous reaction. But that does not mean that the inward flux of reactants into the catalyst is non-existent. In fact, for a fast reaction inside the catalyst particle, the inward flux or consumption of reactants would be much higher. Though the net volume of catalyst particles is small compared to that of bulk solution, the extent of reaction inside the catalyst particles is substantial and even more compared to that of the homogeneous reaction in the bulk. The present model obtains the overall reaction rate assuming that reaction occurs inside the catalyst particle and also in the bulk solution.

3. Modeling

The assumptions involved in developing the model are as follows:

- The catalyst particles are assumed to be spherical in shape with internal pores.
- The swelling of catalyst particles is considered to be negligible.

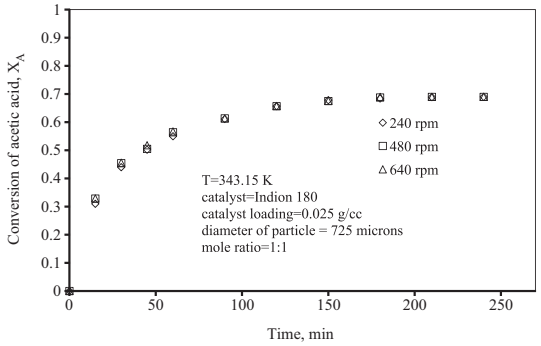

Fig. 3. Kinetics of conversion of acetic acid at various agitation speeds.

- The reactants can react in the bulk solution as well as inside the catalyst particle. Acetic acid and methanol diffuse into the catalyst where the reaction occurs due to catalytic activity. The produced methyl acetate and water diffuse back into the bulk solution.
- The mass transfer resistance external to the catalyst particle is neglected since there is no stagnant film surrounding a catalyst particle due to high stirring.
- The diffusivities of the reactants and products inside the catalyst particle are important. Though they depend on temperature and local concentration, they are assumed to be same for all species and the value is evaluated at an average temperature pertaining to experimental range.
- The volume of solution held within the catalyst particles is assumed to be negligible compared to the bulk solution.
- The volumetric change of solution due to reaction is assumed to be negligible.

The overall rate of reaction could be represented as in Eq. (2).

$$\frac{dN_{Ab}}{dt} = -N_P 4\pi R_P^2 J_A|_{r=R_P} + r_{Ab}V \tag{2}$$

where N_{Ab} is the number of moles of A in the bulk solution at a given time. The time derivative dN_{Ab}/dt represents the rate of change of number of moles of A in the bulk solution where it is measured for concentration changes. N_p is the number of catalyst particles, R_p is the radius of catalyst particles and $4\pi R_p{}^2$ represents the surface area of each catalyst particle. $J_A|_{r=R_p}$ represents the inward flux of acetic acid into the catalyst at its surface. r_{Ab} is the rate of homogeneous reaction in the bulk solution which occurs simultaneously. It primarily depends on temperature but its rate is slow compared to the rate of catalytic reaction inside the catalyst. V is the volume of reaction mixture.

Ideally, the reaction volume needs to be divided with the number of catalyst particles N_p, so that a unit reaction volume could be considered around each catalyst particle. If the quasi steady state approach has to be relaxed, then one needs to solve the transient diffusion–reaction equation inside the catalyst particle as well as outside the catalyst particle. But, by maintaining sufficiently high RPM in the batch reactor, it is found that the rate of reaction does not vary for RPM greater than 240 as could be inferred from Fig. 3. Due to this, the homogeneous part of the reaction occurs uniformly in the bulk solution without any concentration accumulation of the reactants and products. Hence, the external mass transfer resistance surrounding a catalyst particle could be neglected. The schematic of the concentration profile of A inside the catalyst particle and in its neighborhood bulk solution is shown in Fig. 4.

Generally the rate of homogeneous reaction could be represented by Eq. (3) (Fogler, 1995).

$$r_{Ab} = -(k_{f1}C_{Ab}C_{Bb} - k_{b1}C_{Cb}C_{Db}) \tag{3}$$

where k_{f1} is the forward reaction rate constant and k_{b1} is the backward reaction rate constant. C_{Ab}, C_{Bb}, C_{Cb} and C_{Db} are the concentrations in mol/l in the bulk solution.

Conversion of A in the bulk solution is defined as

$$X_A = 1 - \frac{C_{Ab}}{C_{Ao}} \tag{4}$$

Eq. (3) could be simplified as follows in terms of conversion of A:

$$r_{Ab} = -k_{f1}C_{A0}^2\left[(1-X_A)^2 - \frac{X_A^2}{K_e}\right] \tag{5}$$

where $K_e = k_{f1}/k_{b1}$. In experiments it is found that $K_e = 4.95$ from equilibrium data, that is $K_e = X_{Ae}^2/(1-X_{Ae})^2$, where X_{Ae} is equilibrium conversion of acetic acid.

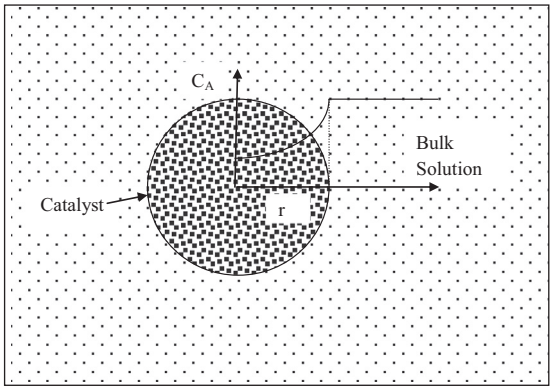

Fig. 4. Schematic of the concentration profile of acetic acid inside the catalyst particle and in the bulk solution.

Now, the first term in Eq. (2) due to flux of A into the catalyst particle could be simplified by the following transformation in terms of reaction conditions that are catalyst loading w_c and radius of catalyst particle R_p.

$$N_P 4\pi R_P^2 = \frac{N_P((4/3)\pi R_P^3)\rho_P}{V}\frac{3V}{R_P\rho_P} = \frac{m_{cat}}{V}\frac{3V}{R_P\rho_P} = w_c\frac{3V}{R_P\rho_P} \tag{6}$$

where m_{cat} is total mass of catalyst, R_p is the radius of catalyst particle in m, ρ_p is the true density of catalyst particle in g/cc and w_c is the catalyst loading in g/cc. The inward flux of acetic acid, $J_A|_{r=R_p}$ at catalyst surface is represented as below (Bird et al., 2002).

$$J_A = D_A\left.\frac{\partial C_A}{\partial r}\right|_{r=R_P} \tag{7}$$

where D_A is the diffusivity of A inside the catalyst particle. This flux has to be obtained by solving reaction–diffusion equation inside the catalyst particle as given below.

$$\frac{\partial C_A}{\partial t} + \underline{\nabla}\cdot\underline{n}_A = \varepsilon r_A \tag{8}$$

where C_A is the concentration of the acetic acid at a location r and time t inside the catalyst particle and ε is the porosity of the catalyst particle. The porous volume of the catalyst particle is filled with the reactant and product liquids. The vector $\underline{n}_A$ is the total molar flux of A due to convection and diffusion as given below in Eq. (9).

$$\underline{n}_A = (\sum \underline{n}_i)x_A + \underline{J}_A \tag{9}$$

here $(\sum \underline{n}_i)$ is the vector sum of molar fluxes of all components, x_A is the mole fraction of acetic acid and J_A is the molecular diffusion flux. If we assume that the reaction proceeds according to stoichiometry then $(\sum \underline{n}_i)=0$ which implies that equimolar counter diffusion of reactants and products occurs inside the catalyst particle. Hence: the flux of A inward into the particle is equal to flux of B and of opposite sign with respect to C and D. Now, the total flux of A in Eq. (9) is given by J_A itself which in turn is as given below in Eq. (10) according to Fick's law of diffusion.

$$\underline{J}_A = -D_A\frac{\partial C_A}{\partial r} \tag{10}$$

The reaction rate inside the catalyst may be assumed as follows

$$r_A = -(k_{f2}C_AC_B - k_{b2}C_CC_D) \tag{11}$$

where C_A, C_B, C_C and C_D are local concentrations inside the catalyst particle. k_{f2} and k_{b2} are the forward and backward reaction rate constants which are different from those of homogeneous

reaction. Note that C_A is inside the catalyst and C_{Ab} is in the bulk solution.

By substituting Eqs. (9)–(11) in Eq. (8), it gives the following equation,

$$\frac{\partial C_A}{\partial t} - D_A \nabla^2 C_A = -\varepsilon[k_{f2} C_A C_B - k_{b2} C_C C_D] \tag{12}$$

here, a pseudo-homogeneous rate equation is used because the pore volume is utilized instead of the pore surface area. In spherical coordinates Eq. (12) becomes

$$\frac{\partial C_A}{\partial t} = D_A \frac{1}{r^2}\frac{\partial}{\partial r}\left(r^2 \frac{\partial C_A}{\partial r}\right) - \varepsilon[k_{f2} C_A C_B - k_{b2} C_C C_D] \tag{13}$$

By using non-dimensionalization as $t^*=t/\tau$, $r^*=r/R_P$, $C_A^*=C_A/C_{A0}$ and by assuming the reactants and products to be consumed and formed in stoichiometric ratio, that is $C_B=C_A$, $C_C=C_{A0}-C_A$, $C_D=C_{A0}-C_A$, Eq. (13) gets transformed as,

$$\frac{\partial C_A^*}{\partial t^*} = \frac{1}{r^{*2}}\frac{\partial}{\partial r^*}\left(r^{*2}\frac{\partial C_A^*}{\partial r^*}\right) - \frac{\varepsilon k_{f2} C_{A0} R_P^2}{D_A}\left[C_A^{*2} - \frac{(1-C_A^*)^2}{K_e}\right] \tag{14}$$

where $\tau=R_p{}^2/D_A$ and $K_e=k_{f2}/k_{b2}$.

By solving Eq. (14) with boundary conditions as $(\partial C_A{}^*/\partial r^*)=0$ at $r^*=0$ and $C_A{}^*=C_{Ab}/C_{A0}=1-X_A$ at $r^*=1$ and initial condition as $t^*=0$, $C_A{}^*=0$ for $0<r^*<1$ inside the catalyst particle, we could determine the inward flux of A at catalyst surface as

$$J_A = \frac{D_A C_{A0}}{R_P}\frac{\partial C_A{}^*}{\partial r^*}\Big|_{r^*=1} \tag{15}$$

By substituting Eqs. (15), (6) and (5) in Eq. (2), it gives the overall reaction rate in terms of conversion of acetic acid as

$$\frac{dX_A}{dt} = w_C\left(\frac{3D_A}{R_P^2\rho_P}\right)\left(\frac{\partial C_A{}^*}{\partial r^*}\right)\Big|_{r^*=1} + C_{A0}k_{f1}\left[(1-X_A)^2 - \frac{X_A^2}{K_e}\right] \tag{16}$$

It is assumed that the equilibrium constant K_e is same for both homogeneous reaction as well as for reaction inside the catalyst particle. It is also assumed that the diffusion constant of acetic acid is similar in magnitude to that of other reactants and products. The variation of diffusion constant with temperature is also assumed to be negligible in the range of operating temperature which otherwise would complicate the reaction–diffusion equation, Eq. (14).

The diffusivity of the acetic acid could be modeled to be dependent on temperature through Wilke–Chang equation in the form of $D_{AB}=1.173\times10^{-16}(\Phi M_B)T/(\mu_B v_A{}^{0.6})$ which predicts the diffusivity of the limiting reactant that is acetic acid in other species namely methanol, water and methyl acetate (Treybal, 1981). An average value of the diffusivity is taken at 10^{-9} m^2/s inside the pores of the catalyst. This is arrived at after taking the effect of porosity also into consideration (Ju et al., 2011).

Now Eq. (16) has to be utilized for predicting the conversion kinetics X_A *versus* time for any given reaction conditions of catalyst loading w_c, temperature T and radius of catalyst particle R_P for RPM > 240. Since there are unknown parameters such as k_{f1}, K_e and k_{f2}, these could be obtained from initial rate of reaction and final equilibrium conversion.

From Eq. (16) it can be seen that the initial reaction rate as $t\to 0$ is a linear function of catalyst loading w_c. Eq. (16) could be rewritten as below for $t\to0$

$$\left.\frac{dX_A}{dt}\right|_{t\to0} = \beta w_C + C_{A0}k_{f1} \tag{17}$$

The initial rate of conversion of acetic acid is plotted in Fig. 5 against catalyst loading to obtain slope and intercept for various temperatures with average diameter of catalyst particle, $d_P=725$ μm.

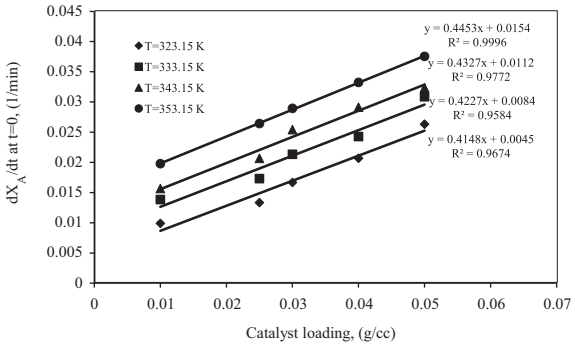

Fig. 5. Linear fit for initial reaction rate *versus* catalyst loading. The diameter of catalyst particles in all the experiments is 725 μm.

Table 2
Reaction rate constants k_{f1} and k_{f2} at different temperatures.

Temperature (K)	k_{f1} (l/mol min)	k_{f2} (l/mol min)
323.15	0.000391	0.148
333.15	0.000781	0.1515
343.15	0.00108	0.156
353.15	0.001516	0.1615

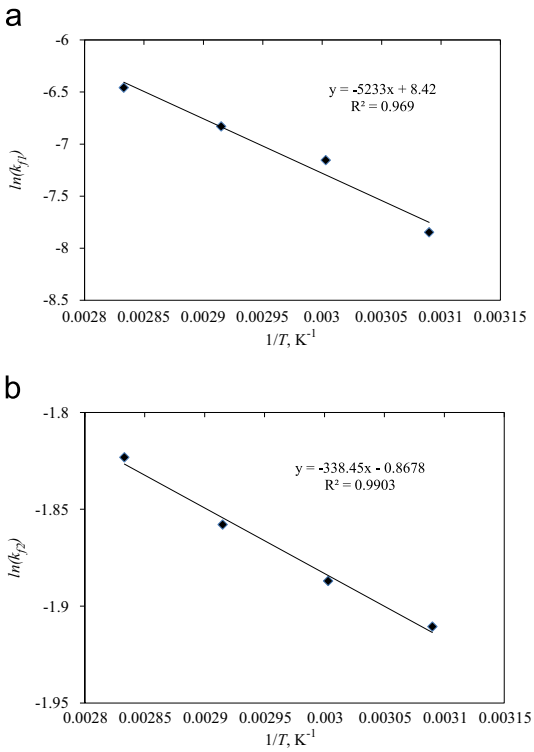

Fig. 6. (a) Arrhenius plot for homogeneous reaction rate constant in bulk solution. (b) Arrhenius plot for reaction rate constant inside catalyst pores.

From y-intercept value, k_{f1} is inferred and shown in Table 2. Similarly β, the slope in Eq. (17) is used to find the initial non-dimensional flux of A at surface of catalyst particle as $(\partial C^*{}_A/\partial r^*)|_{r^*=1}$ which is part of the first term in Eq. (16). Now, Eq. (14), the reaction–diffusion equation inside catalyst particle is solved to find k_{f2} such that this surface flux is matched. The obtained values of k_{f2} are shown in Table 2.

An Arrhenius equation is fitted for representing variation of k_{f1} and k_{f2} with respect to temperature T as shown in Fig. 6(a) and (b).

Arrhenius equation in general form is given by

$$k_f = k_{f0}\exp\left(-\frac{E_f}{RT}\right) \quad (18)$$

where k_{fo} is pre-factor and E_f is the activation energy. The obtained expressions are $k_{f1}=4536\ \exp\ (-43507/(RT))$ l/mol min and $k_{f2}=0.421\ \exp\ (-2813/(RT))$ l/mol min. The equilibrium constant K_e is obtained from equilibrium conversion as 4.95 for all temperatures. The equilibrium constant K_e value as found in literature are: 3.9–9.0 (Jagadeesh Babu et al., 2011; Tsai et al., 2011).

The regressed parameters β and $C_{A0}k_{f1}$ after a linear fit of Eq. (17) exhibit an R-square value of above 0.95 as shown in Fig. 5. Since it is a good linear fit, the model is justified. The term dX_A/dt in Eq. (17) could have an error due to estimation of the conversion X_A of acetic acid. It is nearly 2% since it is calculated from the concentration C_A which in turn depends on titre value of NaOH solution rundown. The measurement of titre value could have an error of 0.1 ml. The measured temperature could have an error of 1 °C. The catalyst loading could have an error of 0.001 g/cc. The reactants weight could have an error of 0.1 g.

In this kinetic model, it is considered that the void volume inside the catalyst particles is also utilized for the reaction. The liquid species can penetrate into the pore volume of the catalyst particle by diffusion. The reaction rate constant could be much higher in the pore volume of the catalyst particle since active sites are dense. In other words, the H^+ ion concentration that catalyzes the reaction is higher in the pores than in the bulk liquid outside the particle. Due to the constraint of charge neutrality, the entire H^+ ion content of the catalyst particle would not be dissolved into the bulk reactant liquid. Nevertheless, the presence of catalyst increases the homogeneous rate constant as well because the liberated H^+ ions from the catalyst. Hence, in this catalytic reaction, both the homogeneous and heterogeneous rate constants are fitted simultaneously from the initial reaction rate data. In view of the above condition, the net reaction rate due to catalytic activity substantially occurs inside the catalyst particles. In addition to it, there is the homogeneous reaction occurring in the bulk reactant solution. Hence there are two rate constants and one equilibrium constant as parameters in the model. Further, these parameters depend on temperature through Arrhenius type models as discussed earlier.

The contributions of heterogeneous and homogeneous reactions towards conversion are represented by first and second terms respectively of Eq. (16). Hence, the model parameters are fitted using only the initial reaction rate and equilibrium conversion. The rest of the kinetics is predicted using those parameters. The experiment provides the overall conversion of acetic acid due to homogeneous and heterogeneous reactions. The individual rate constants could be determined in a coupled model only rather than individually. There are few homogeneous models like in the case of H_2SO_4 catalyzed esterification of acetic acid with methanol. But those rate constants cannot be applied for the ion exchange resin catalyzed esterification.

In order to estimate the internal diffusion effect, Weisz modulus for catalytic reactions in solid catalyst particles could be quantified but the present situation has reaction occurring in the bulk as well. Therefore, it may not be appropriate to calculate Weisz modulus for esterification reaction using ion exchange resin catalyst particles. Instead, the contribution of heterogeneous and homogeneous reactions towards conversion is represented by first and second terms respectively of Eq. (16). The conversion X_A contributed by homogeneous part and heterogeneous part could be compared. Nevertheless, the Weisz modulus is obtained as 1.42 at initial time for reaction conditions such as temperature=323.15 K, catalyst loading=0.025 g/cc and catalyst particle size of 725 μm. Since it is greater than 1, the internal diffusion is important (Fogler, 1995; Ju et al., 2011). Weisz–Prater parameter is given by $C_{w\text{-}p}=r_{obs}\rho_p R_p^2/(D_A C_{Ao})$.

For reaching a conclusion on "pore diffusion based model", assumptions are made in simplifying the equations as much as possible but retaining the features that there is diffusion into the catalyst particles and a simultaneous reaction occurring there. These assumptions have provided a solvable Eq. (14) and the final results would confirm the applicability of "pore diffusion based model".

4. Simulation

The algorithm implemented for obtaining time evolution of conversion of acetic acid is shown in Fig. 7. Eq. (14) is solved at every time step and Eq. (16) is used to update and predict the overall kinetics of conversion of acetic acid X_A *vs* time. A quasi steady state approach is adopted. The time step used for Eq. (14) is 2 min where as the time step used for Eq. (16) is 15 min.

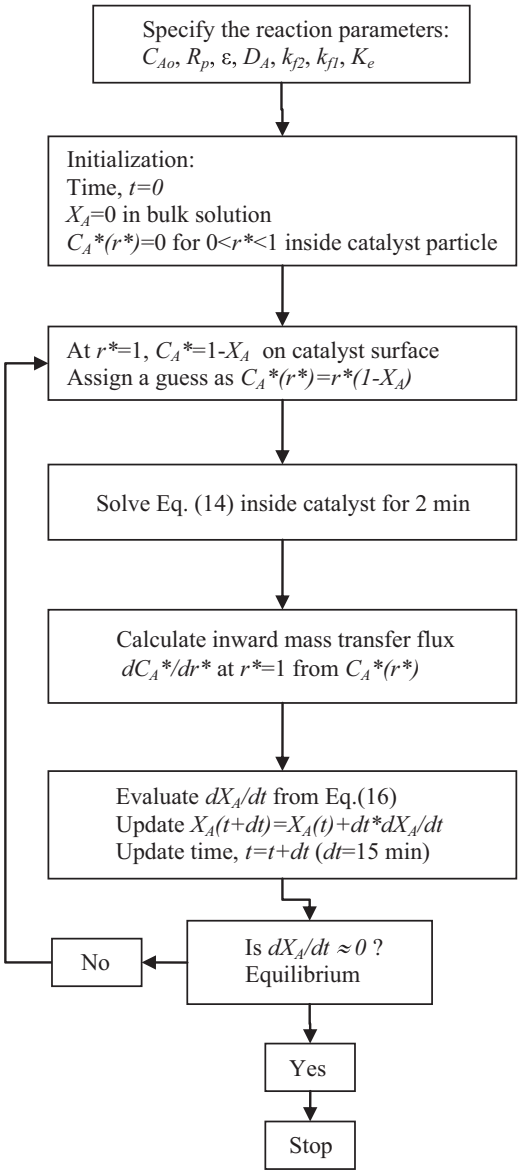

Fig. 7. Schematic flow diagram of the algorithm implemented for simulation of the model to predict the overall conversion kinetics.

The time scale of diffusion inside the particle is of the order of R_P^2/D_A where R_p is the radius of the particle and D_A is the diffusivity of the acetic acid inside the pores containing the mixture of reactants and products. Let the average radius of the catalyst particle be $R_p=400$ μm and pore diffusivity be 10^{-9} m^2/s. This time scale comes to approximately $(400\times10^{-6})^2/10^{-9}=160$ s. In the outer film, assuming it also to be of the thickness of R_p, the diffusion time scale is $(400\times10^{-6})^2/10^{-8}=16$ s. Here, for the bulk solution, diffusivity is assumed to be 10^{-8} m^2/s which is higher than in pores. Hence, even if the external film exists, the internal pore diffusion resistance is higher. This also gives an indication of the time scale one needs to use for updating the concentration distribution inside the catalyst particle. The above discussion indicates that the concentration distribution inside the catalyst particles reaches quasi steady sate in 2–3 min. Now the time scale for updating the bulk concentration has to be at least 2–3 min. In the experiment, the concentration of acetic acid is measured for every 15 min. Hence this true time step could be used in the simulation which would give a coarse result. But one could use the time step of above 2–3 min minimum. The simulation time is counted only from the cumulative of the time steps used for updating the bulk concentrations. The 2–3 min time duration used for solving Eq. (14) as a sub-routine is only for the purpose of finding the inward flux of acetic acid at surface of the catalyst particle.

From the simulation of diffusion inside the catalyst particle, we need to calculate the inward flux of acetic acid at surface which would be multiplied with surface area of the catalyst particle. In principle the hybrid model of homogeneous and heterogeneous reaction could be simulated for the arrangement in Fig. 4 by using COMSOL Multiphysics software. But the drawback is that it would bring in the concentration gradient in the bulk as well. It is difficult to formulate well mixed condition in bulk solution. On the other hand MATLAB Software could be used to solve Eq. (14) in dimensionless form for 2–3 min which will provide the inward flux of acetic acid on catalyst particle surface during that time interval. And for that duration, the bulk concentration of acetic acid is taken as its latest value from previous iteration. Hence a multi time-scale model is used since the reaction is slow in the bulk but inside the catalyst the concentrations reaches steady state fast. Hence, it is a quasi steady state model.

The parameters used for solving Eq. (14) are: $D_A=6\times10^{-8}$ m^2/min, $k_{f1}=4536\exp(-43507/(RT))$ l/mol min, $k_{f2}=0.421\exp(-2813/(RT))$ l/mol min, $C_{A0}=10.24$ mol/l, $K_e=4.95$, $\rho_p=1.242$ g/cc, T is temperature in Kelvin scale and R is gas constant, 8.314 J/mol K

We have assumed a linear concentration profile initially inside the catalyst particle with boundary setting as: at $t^*=0$, $r^*=0$, $C_A^*=0$ and at $t^*=0$, $r^*=1$, $C_A^*=C_{Ab}^*$.

Eq. (14) is solved in MATLAB software as an unsteady state one-dimensional partial differential equation. For one particular temperature, w_c and R_p, the concentration distribution inside the catalyst particle is plotted as a function of time shown in Fig. 8a. The contributions of homogeneous part and heterogeneous part to overall reaction kinetics are shown in Fig. 8b. It is convincing that the model assumption of reaction occurring inside the catalyst particle is valid. From this figure, it is evident that the heterogeneous part of conversion is substantial.

The predicted kinetics based on Eq. (16) for conversion of acetic acid with respect to time is compared with experimental data as shown in Figs. 9–11. There is a good agreement between the experimental data and theoretical model. The negligible effect of particle size on reaction kinetics is because the entire volume of catalyst is utilized for heterogeneous reaction instead of only the outer surface. Hence, as long as catalyst loading is same, the variation of particle size does not change the total volume of the catalyst. Thus, the pore diffusion model accounts for the effect of catalyst loading, temperature and diameter of particle explicitly.

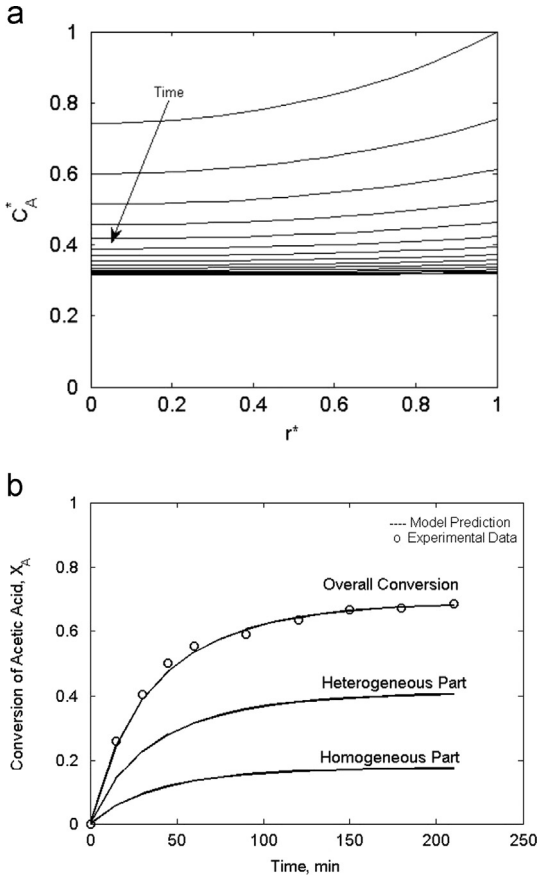

Fig. 8. (a) Dimensionless concentration distribution of acetic acid inside the catalyst particle at different times for every 15 min. The reaction conditions are diameter of particle=725 μm, catalyst loading=0.025 g/cc and temperature=333.15 K. (b) Quantitative representation of contribution of homogeneous and heterogeneous reactions towards overall conversion of acetic acid. The reaction conditions are diameter of particle=725 μm, catalyst loading=0.025 g/cc and temperature=333.15 K.

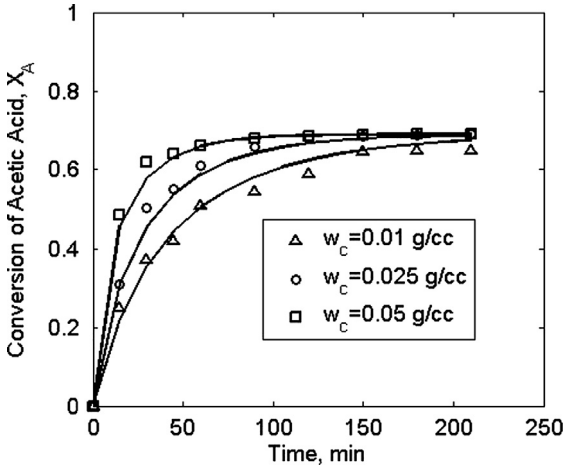

Fig. 9. Conversion kinetics of acetic acid at different catalyst loadings at 343.15 K. The catalyst particle size=725 μm. Solid line represents model prediction.

5. Conclusions

In this paper, a hybrid model for heterogeneous catalytic esterification of acetic and methanol is developed. The proposed model takes into the account that the reaction occurs inside the catalyst particle as well as in the homogeneous reaction occurring in the bulk liquid. The convection-diffusion-reaction equation in a

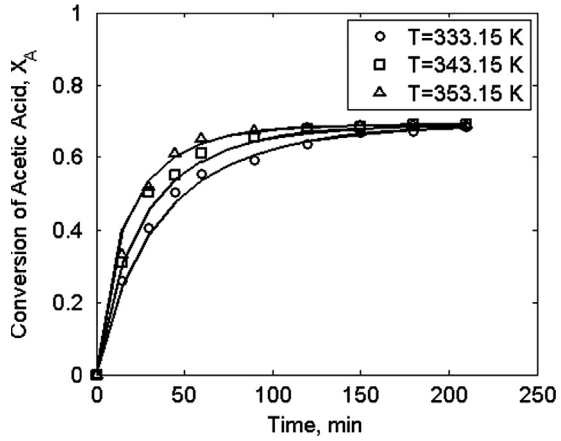

Fig. 10. Conversion kinetics of acetic acid at different temperatures at 0.025 g/cc catalyst loading and with catalyst particle size of 725 μm. Solid line represents model prediction.

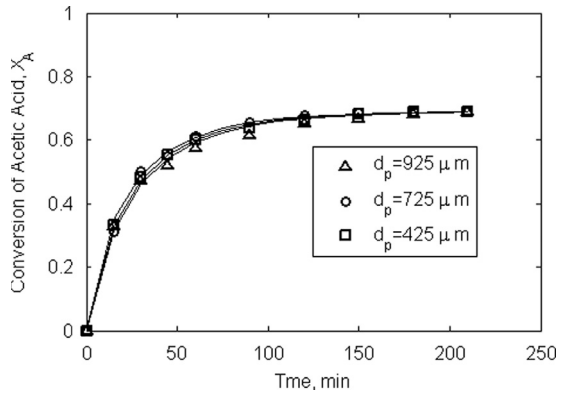

Fig. 11. Conversion kinetics of acetic acid for different catalyst particle sizes at temperature of 343.15 K and 0.025 g/cc catalyst loading. Solid line represents model prediction.

porous spherical catalyst particle has been solved using MATLAB numerical tools. A multi time scale approach or a quasi steady state approach has been adopted for numerical integration of rate equation. A small time step is assumed for solving the diffusion-reaction equation inside the catalyst particle and large time step is used for updating the concentration or conversion in the bulk solution. The model predicts the kinetics of conversion accurately for various reaction conditions such as catalyst loading, temperature and diameter of particle. The two features, that are: explicit accounting for catalyst loading and particle diameter of the model are novel aspects compared to the literature models. In most of the existing literature, the rate constant is fitted to a polynomial function of catalyst loading based on pseudo-homogeneous assumption. In the present model, the catalyst loading and diameter of the particle are introduced through a phenomenological modeling approach.

Nomenclature

C_{A0}	acetic acid concentration in initial reaction mixture (mol/l)
C_{Ab}	acetic acid concentration in the bulk solution (mol/l)
C_{Bb}	methanol concentration in the bulk solution (mol/l)
C_{Cb}	methyl acetate concentration in the bulk solution (mol/l)
C_{Db}	water concentration in the bulk solution (mol/l)
C_A	acetic acid concentration in catalyst (mol/l)
C_B	methanol concentration in catalyst (mol/l)
C_C	methyl acetate concentration in catalyst (mol/l)
C_D	water concentration in catalyst (mol/l)
C_A^*	dimensionless concentration of acetic acid in catalyst
C_{w-p}	Weisz–Prater parameter
D_A	diffusion coefficient of acetic acid in catalyst (m^2/min)
d_p	diameter of catalyst particle (m)
E_f	activation energy (J/mol)
J_A	diffusional flux of acetic acid (kmol/m^2 min)
K_e	equilibrium constant
k_{f1}	forward homogeneous reaction rate constant (l/mol min)
k_{b1}	backward homogeneous reaction rate constant (l/mol min)
k_{f2}	forward heterogeneous reaction rate constant (l/mol min)
k_{b2}	backward heterogeneous reaction rate constant (l/mol min)
k_{f0}	frequency factor in rate constant (l/mol min)
M_B	molecular weight of B (g/mol)
m_{cat}	mass of catalyst (g)
$\underline{n}_A$	total molar flux of acetic acid in the catalyst particle (kmol/m^2 min)
$\underline{n}_i$	total molar flux of species 'i' in the catalyst particle (kmol/m^2 min)
N_{Ab}	number of moles of acetic acid in bulk solution (mol)
N_P	number of catalyst particles
r	radial location in particle (m)
r^*	dimensionless radial location in catalyst
r_A	reaction rate of acetic acid in catalyst (mol/l min)
r_{Ab}	reaction rate of acetic acid in bulk solution (mol/l min)
r_{obs}	initial reaction rate (mol/g min)
R	gas constant (J/mol K)
R_P	radius of particle (m)
T	absolute temperature (K)
t	time (min)
t^*	dimensionless time
v_A	molar volume of A (m^3/kmol)
V	volume of reaction mixture (l)
w_c	catalyst loading (g/cc)
X_A	acetic acid conversion
X_{Ae}	acetic acid conversion at equilibrium
β	slope of initial conversion rate *versus* catalyst loading (1/min.(g/cc))
ε	porosity or void fraction inside catalyst particle
μ_b	viscosity of species B (N s/m^2)
ϕ	association factor
ρ_p	density of catalyst particles (g/cc)
τ	diffusional time scale (min)

References

Agreda, V.H., Partin, L.R., Heiss, W.H., 1990. High purity methyl acetate via reactive distillation. Chemical Engineering and Processing 86 (2), 40–46.
Ali, S.H., Tarakmah, A., Merchant, S.Q., Al-Sahhaf, T., 2007. Synthesis of esters: development of the rate expression for the Dowex 50 Wx8-400 catalyzed esterification of propionic acid with 1-propanol. Chemical Engineering Science 62, 3197–3217.
Bird, R.B., Stewart, W.E., Lightfoot, E.N., 2002. Transport Phenomena, second ed. John Wiley & Sons.
Chakrabarti, A., Sharma, M.M., 1993. Cationic ion exchange resins as catalyst. Reactive Polymers 20, 1–45.
Cruz, V.J., Izquierdo, J.F., Cunill, F., Tejero, J., Iborra, M., Fite, C., Bringue, R., 2007. Kinetic modelling of the liquid-phase dimerization of isoamylenes on Amberlyst 35. Reactive and Functional Polymers 67 (3), 210–224.
Delgado, P., Sanz, M.T., Beltran, S., 2007. Kinetic study for esterification of lactic acid with ethanol and hydrolysis of ethyl lactate using an ion-exchange resin catalyst. Chemical Engineering Journal 126, 111–118.
Ehteshai, M., Rahimi, N., Eftekhari, A.A., Nasir, M.J., 2006. Kinetic study of catalytic hydrolysis reaction of methyl acetate to acetic acid and methanol. Iranian Journal of Science and Technology 30 (5), 595–606.

Fogler, H.S., 1995. Elements of Chemical Reaction Engineering, second ed. Prentice Hall India, New Delhi.
Jagadeesh Babu, P.E., Sandesh, K., Saidutta, M.B., 2011. Kinetics of esterification of acetic acid with methanol in the presence of ion exchange resin catalysts. Industrial and Engineering Chemistry Research 50, 7155–7160.
Ju, I.B., Lim, H.W., Jeon, W., Suh, D.J., Park, M.J., Suh, Y.W., 2011. Kinetic study of catalytic esterification of butyric acid and *n*-butanol over Dowex 50Wx8-400. Chemical Engineering Journal 168, 293–302.
Kirbaslar, S.I., Baykal, Z.B., Dramur, U., 2001a. Esterification of acetic acid with ethanol catalysed by an acidic ion-exchange resin. Turkish Journal of Engineering and Environmental Science 25, 569–577.
Kirbaslar, S.I., Terzioglu, H.Z., Dramur, U., 2001b. Catalytic esterification methyl alcohol with acetic acid. Chinese Journal of Chemical Engineering 9 (1), 90–96.
Liu, Y., Lotero, E.J., Goodwin Jr., J.G., 2006. A comparison of the esterification of acetic acid with methanol using heterogeneous *versus* homogeneous acid catalysis. Journal of Catalysis 242, 278–286.
Lopez, D.E., Suwannakarn, K., Goodwin Jr., J.G., Bruce, D.A., 2008. Reaction kinetics and mechanism for the gas- and liquid-phase esterification of acetic acid with methanol on tungstated zirconia. Industrial and Engineering Chemistry Research 47, 2221–2230.
Mao, W., Wang, X., Wang, H., Chang, H., Zhang, X., Han, J., 2008. Thermodynamic and kinetic study of tert-amyl methyl ether (TAME) synthesis. Chemical Engineering and Processing: Process Intensification 47, 761–769.
Popken, T., Steinigeweg, S., Gmehling, J., 2001. Synthesis and hydrolysis of methyl acetate by reactive distillation using structured catalytic packings: experiments and simulation. Industrial and Engineering Chemistry Research 40, 1566–1574.
Popken, T., Gotze, L., Gmehling, J., 2000. Reaction kinetics and chemical equilibrium of homogeneously and heterogeneously catalyzed acetic acid esterification with methanol and methyl acetate hydrolysis. Industrial and Engineering Chemistry Research 39, 2601–2611.
Rolfe, C., Hinshelwood, C.N., 1934. The kinetics of esterification: the reaction between acetic acid and methyl alcohol. Transactions of the Faraday Society 30, 935–944.
Ronnback, R., Salmi, T., Vuori, A., Haario, H., Lehtonen, J., Sundqvist, A., Tirronen, E., 1997. Development of a kinetic model for the esterification of acetic acid with methanol in the presence of a homogeneous acid catalyst. Chemical Engineering Science 52, 3369–3381.
Song, W., Venimadhavan, G., Manning, J.M., Malone, M.F., Doherty, M.F., 1998. Measurement of residue curve maps and heterogeneous kinetics in methyl acetate synthesis. Industrial and Engineering Chemistry Research 37, 1917–1928.
Treybal, R.E., 1981. Mass Transfer Operations, third ed. McGraw Hill.
Tsai, Y.T., Lin, H.M., Lee, M.J., 2011. Kinetic behavior of esterification of acetic acid with methanol over Amberlyst 36. Chemical Engineering Journal 171, 1367–1372.
Titus, M.P., Bausach, M., Tejero, J., Iborra, M., Fite, C., Cunill, F., Izquierdo, J.F., 2007. Liquid-phase synthesis of isopropyl tert-butyl ether by addition of 2-propanol to isobutene on the oversulfonated ion-exchange resin Amberlyst-35. Applied Catalysis A: General 323, 38–50.
Winkler, E.B., Gmehling, J., 2006. Transesterification of methyl acetate and *n*-butanol catalyzed by Amberlyst 15. Industrial and Engineering Chemistry Research 45, 6648–6654.
Yadav, G.D., Mehta, P.H., 1994. Heterogeneous catalysis in esterification reactions: preparation of phenethyl acetate and cyclo-hexyl acetate by using a variety of solid acidic catalysts. Industrial and Engineering Chemistry Research 33, 2198–2208.
Yadav, G.D., Thathagar, M.B., 2002. Esterification of maleic acid with ethanol over cation-exchange resin catalysts. Reactive and Functional Polymers 52, 99–110.
Yu, W., Hidajat, K., Ray, A.K., 2004. Determination of adsorption and kinetic parameters for methyl acetate esterification and hydrolysis reaction catalyzed by Amberlyst 15. Applied Catalysis A: General 260, 191–205.
Zhang, Y., Ma, L., Yang, J., 2004. Kinetics of esterification of lactic acid with ethanol catalyzed by cation-exchange resins. Reactive and Functional Polymers 61 (1), 101–114.